Asociación Argentina
de Mecánica Computacional

Mecánica Computacional Vol XXXI, págs. 405-418 (artículo completo)
Alberto Cardona, Paul H. Kohan, Ricardo D. Quinteros, Mario A. Storti (Eds.)
Salta, Argentina, 13-16 Noviembre 2012

OPTIMIZATION OF ACOUSTIC DOPPLER VELOCIMETER SAMPLING STRATEGIES USING DIRECT NUMERICAL SIMULATION OF TURBULENCE FLOW

Vicente G. Gil Montero[a], Carlos M. García[a] and Mariano I. Cantero[b]

[a]*Laboratorio de Hidráulica, FCEFyN, Universidad Nacional de Córdoba, Av. Filloy s/n, Ciudad Universitaria Córdoba, Argentina, gastongilmontero@gmail.com,*
http://www.efn.uncor/investigacion/DETU

[b]*Consejo Nacional de Investigaciones Científicas y Técnicas (CONICET),*
División de Mecánica Computacional, Centro Atómico Bariloche, Comisión Nacional de Energía Atómica

Instituto Balseiro, Universidad Nacional de Cuyo, Comisión Nacional de Energía Atómica

Keywords: turbulence, acoustic Doppler velocimeter, direct numerical simulation (DNS).

Abstract. The experimental characterization of turbulent flows requires flow velocity measurements with high temporal and spatial resolutions. This information is generally used in studies and projects related to the determination of the mean velocity flow field, the coefficient of mass transfer between the liquid and suspended particles (sediment, bubbles), rates of agglomeration of suspended solids, calculation of rates of mass transfer between the liquid and the walls (erosion), etc. The Acoustic Doppler Velocimeter (ADV) meets these requirements and it has been widely used as an experimental device for measuring turbulent flows in the last two decades. The operating principle of the ADV is based on the determination, with high temporal resolution, of the three flow velocity components in a small sampling volume, whose geometry can be modified by the user. Part of the internal signal preprocessing performed in this technology involves temporal and spatial averaging of the measured data to minimize noise. This work aims to analyze the effects of the internal processing and measurement configuration selected by the user on the estimated parameters characterizing the flow turbulence. To achieve this objective, turbulent channel flow fields simulated with direct numerical simulation were sampled using different sampling strategies simulating the ADV performance. The results show the relative significance of the filtering effects on turbulence parameters such as mean velocity, turbulence fluctuations, Reynolds stresses, and turbulent kinetic energy for different ADV sampling strategies.

1 INTRODUCTION

The acoustic Doppler velocimeters are able to report with high precision mean values of the flow velocities in three directions (Kraus et al. 1994; Lohrmann et al. 1994; Anderson and Lohrmann 1995; Voulgaris and Trowbridge et al.1998; Lane et al. 1998; López and García (2001) even in flows with low velocities (Lohrmann et al. 1994). Nevertheless its employment to characterize turbulence requires considering some important aspects (Nikora and Goring 1998, Goring and Nikora 2002, García et al. 2005, Rusello et al. 2006) as the range of flow velocities and flow depths.

Recently most of the research aimed to analyze the capability of the acoustic Doppler velocimeters to characterize the flow turbulence (specifically the turbulent kinetic energy and power spectrum) had been focused in the noise of the recorded signals and the way to remove it (Lohrmann et al. 1994, Anderson et al. 1995, Voulgaris et al. 1998, Lemmin et al. 1999, Mc Lelland et al. 2000, Romagnoli et al. 2010). Indeed there are a lacks of works addressed to evaluate the effects of the internal pre-processing and the sampling configurations selected by the users.

The ADV technology measures the flow field in a remote sampling volume whose dimension may be specified by the users. In order to determine one flow velocity vector in the sampling volume the signal pre-processing of the instrument makes a spatial averaging of all particle velocities within the sampling volume. Then, the ADV technology performs a temporal averaging to minimize the noise in the signal. García et al. (2005) analyzed the temporal averaging performs by the ADV. The mentioned study presents the Acoustic Doppler velocimeter performance curves (APCs) which were introduced to define optimal flow and sampling conditions for measuring turbulence. The APC can be used for the design of experimental measurements, as well as for the interpretation of both field and laboratory observations using acoustic Doppler velocimeters. However, the mentioned analysis only considered the temporal filter performs by the ADV without considering the spatial averaging.

The purpose of this work aims to evaluate the effects of the spatial and temporal averaging on ADV turbulence measurements. Specifically the analysis is oriented to complete the curves presented in García et al. (2005) considering in addition to the temporal averaging, the spatial averaging.

In order to achieve this objective a turbulent channel flow fields was generated using direct numerical simulation. Then the flow field was sampled simulating the ADV pre-processing and adopting different user sampling configurations to developed curves that describe the ADV performance. These curves were then validated with experimental data recorded for this work.

1.1 Principle of operation of Acoustic Doppler Velocimeters

A velocimeter acoustic Doppler measures the three velocities components of the flow velocity vector, using the phase shift between two successive acoustic pulses. The ADV sends two short successive acoustic pulses in a known frequency that broadcasted through water along the instrument axes. Then the signals reflected in the particles suspended in the water are sampled. The phase shift is calculated from the auto and cross correlation computed for each single pulse pair (Son Tek et al. 1997). Then it is used to determine the flow field velocity. Therefore the velocities of the particles are measured, instead of the water velocity; however it is assumed that they are both the same,

$$U = \frac{x_2 - x_1}{T_1} = \frac{\lambda(\phi_2 - \phi_1)}{4\pi T_1} \quad (1)$$

where ϕ_2 *y* ϕ_1 are respectively the phases of the sent and reflected pulses and T_1 is the time interval between both pulses, meanwhile x_1 and x_2 are the particles location when the particles backscatter the acoustic pulses 1 and 2 respectively.

Each pair acoustic transmitter/receiver (the ADV technology uses 1 transmitter and 3 or 4 receivers depending on the model of the selected instrument) defines the projection of the velocity in its own biestetic axes because the trajectory of the pulse does not match between the transmitter and the receiver. The velocities in the three axes are converted through an internal processing module in the main velocities referring to the Cartesian axes XYZ. Consequently the receivers are aligned in such a way that they intercept forming a cylindrical volume, the sampling volume. Nowadays there exist in the market only two companies dedicated to manufacturing this product: Sontek/YSI and Nortek As. Instruments manufactured by both companies present the same sampling volume diameter that is equal to 6 mm (defined by the size of the transmitter), meanwhile the definition of the height of the volume dependent on the company. In the case of Sontek/YSI, the volume height is fixed in 9 mm; on the other hand Nortek As allows the users to define the height between 3mm to 14mm. The sampling volume height is defined by the length of the transmitted pulse and the time that it remains open. Within the sampling volume many particles in movement interact, but only one flow velocity vector is determined what implies that there is a spatial averaging. This is the first averaging perform by the signal preprocessing.

After one unique vector of velocity is determined for the sampling volume, the following step performs by the signal preprocessing is the temporal averaging. Since the instrument employs different frequencies for sampling (f_s) and for recording (f_R) the signal, a temporal average of N values is perform in order to minimize the noise and to smooth out the peaks sampled at $f_R=f_s/N$. For example, for the MicroADV Sontek, the instrument sampling frequency (f_s) is in the range between 100 [Hz] and 263 [Hz] depending on the flow velocity range and the user set frequency (f_R) (see Table 1). This averaging process can be considered as a digital non-recursive filter (Hamming et al. 1983, Bendat et al. 2000, Garcia et al. 2005).

	f_R [Hz]	1	25	100
Velocity range	$f_{cut\text{-}off}$ [Hz]	0.44	11.3	50
[cm/s]	f_s [Hz]			
250		263	250	200
100		256	225	200
30		226	200	100
10		180	125	100
3		143	125	100

Table 1: Number of averaged velocity values (N) by Sontek MicroADV for different sampling configurations (Velocity ranges and recording frequencies).

For the Vectrino Nortek ADV (with the Plus firmware option available), the maximim number of sampled values are 426, 667, 1124, 1754 and 1818 for velocity ranges of 3, 10, 30, 100 and 250cm/s, respectively. The higer sampling rate of Vectrino Nortek ADV is due to the fact that the MicroADV Sontek performs a sequential sampling of each receiver while Vectrino Norte ADV perform a simulatenous sampling for all the the receivers.

In addition to the internal pre-processing of the ADV (temporal and spatial averaging), the turbulence characterization obtained by the ADV technology is affected mainly by other two factors: the sampling and experimental conditions (the measurement location relative to the bottom and the sampling frequency) and noise. The purpose of this work aims to evaluate the effects of the spatial and temporal averaging on ADV turbulence measurements. In order to achieve this objective data sets of three dimensional flow velocities with high temporal and spatial resolution were generated from Direct Numerical Simulation of turbulent open channel flow. As the DNS solves all the relevant time and length scales present in the flow without requiring for a turbulence closure scheme, it provides high resolution flow field velocity data requested for this work. The following section show the mathematical and numerical models used for the flow simulation.

1.2 Mathematical and numerical models

The model consists of a horizontal channel in which the flow is driven by a uniform mean pressure gradient in the streamwise direction (y). The dimensionless set of equations that govern the flow read

$$\frac{\partial \mathbf{V}}{\partial t} + \mathbf{V} \cdot \nabla \mathbf{V} = \mathbf{G} - \nabla p + \frac{1}{Re_\tau} \nabla^2 \mathbf{V} \tag{2}$$

$$\nabla \cdot \mathbf{V} = 0 \tag{3}$$

where V=(u,v,w)=(u_x,u_y,u_z) is the dimensionless velocity vector, p is the dimensionless dynamic pressure and G= (0,1,0) is the negative of the dimensionless mean pressure gradient. Dimensionless variables are defined using (a) the shear velocity, $u^*=(\tau_w/\rho)^{1/2}$, as the velocity scale where τ_w is the bottom wall shear stress and ρ is the fluid density; (b) the channel height, H, as the length scale; (c) $T_t=H/u^*$ as the time scale and (d) $P=\rho u^{*2}$ as the pressure scale. The dimensionless number in equation (2) is the Reynolds number defined as $Re_\tau=u^*H/\nu$ where ν is the dynamic viscosity, and for this work Re_τ=509, which gives a bulk Reynolds number $Re=V_wH/\nu$ = 9164, using the ratio Vw/u^* = 18.

The governing equations are solved using a de-aliased pseudospectral code (Canuto et al., 1988). Fourier expansions are employed for the flow variables in the horizontal directions (y and x are the streamwise and spanwise directions, respectively). In the inhomogeneous vertical direction (z) a Chebyshev expansion is used with Gauss-Lobatto quadrature points. An operator splitting method is used to solve the momentum equation along with the incompressibility condition (see for example Brown et al., 2001). First, an advection-diffusion equation is solved to compute an intermediate velocity field. After this intermediate velocity field is computed, a Poisson equation is solved to compute the pressure field. Finally, a

pressure correction step is performed to obtain the final incompressible velocity field. A low-storage mixed third order Runge-Kutta and Crank-Nicolson scheme is used for the temporal discretization of the advection-diffusion terms. More details of the implementation of this numerical scheme can be found in Cortese and Balachandar (1995). Validation of the code can be found in Cantero et al. (2007a) and Cantero et al. (2007b).

The length of the simulated channel (simulated domain) is $L_y=4\pi H$, the width is $L_x=4/3\pi H$, and the height is $L_z=H$. The grid resolution used is $N_x=256$ x $N_y=256$ x $N_z=129$ and the non-linear terms are computed in a grid $3N_x/2$ x $3N_y/2$ x N_z in order to prevent aliasing errors. The bottom wall represents a smooth no-slip boundary to the flow and the top wall is a free slip wall. Then, the dimensionless boundary conditions employed are,

$$\mathbf{V} = 0 \quad \text{at} \quad z = 0, \tag{4}$$

$$\frac{\partial u}{\partial z} = 0, \quad \frac{\partial v}{\partial z} = 0, \quad \text{and } w = 0 \text{ at } z = 1. \tag{5}$$

The dimensionless integration time (T_i) employed in this work is u*/H=50 (100.000 time steps) after the flow has achieved a statistically steady state. The DNS model was validated by comparing vertical profiles of turbulence parameters for an open-channel flow with experimental results (Nezu et al. 1977 and Nezu and Nakagawa, 1993), and semi-theoretical curves (Nezu and Rodi, 1986, and Nezu and Nakagawa, 1993).

2 METHODOLOGY

2.1 Defining synthetic flow conditions to be sampled using ADV

The mathematical model presented in equations (2) and (3) represents the temporal and spatial evolution of dimensionless variables. The dimensionless number in equation (2) $Re_\tau=u^*H/\nu$ used in the direct numerical simulation is $Re_\tau=509$. In order to define flow conditions to be sampled using ADV, a flow depth equal to 6.41cm has been defined for the analysis. This values of u* = 0.0079 m/s (assuming a value of $\nu = 0.000001$ m^2/s), mean flow velocity = 0.143 m/s, energy slope = 0.0001 and a channel width of 0.134 m has been computed. On the basis of these variables the temporal resolution of the simulated flow field is $\Delta t = 0.004035$ sec (frequency = 247.8 Hz).

2.2 Sampling synthetic flow conditions simulating ADV sampling strategies

Flow velocities were sampled from the DNS data by simulating the ADV measurement strategy. The synthetic velocity data were sampled at different distances from the bottom of the channel, considering different recording frequencies and several size of sampling volumes of ADV in order to represent the main measurement strategies defined by a user and the pre-processing of the instrument. The velocity vector obtained for each volume was calculated as follow,

$$\mathrm{v(x,y,z,t)} = \frac{1}{JKI}\sum_{i=0}^{I-1}\sum_{j=0}^{J-1}\sum_{k=0}^{K-1} u(x+idx, y+jdy, z+kdz, t) \tag{6}$$

Assuming spatial weighting function *h(x,y,z)*,

$$h(x,y,x) = \begin{cases} 1/JKL, & x_c - \frac{L_x}{2} \le x \le \frac{L_x}{2} + x_c;\ y_c - \frac{L_y}{2} \le y \le \frac{L_y}{2} + y_c;\ z_c - \frac{L_z}{2} \le z \le \frac{L_z}{2} + z_c \\ 0, & else\ \ where \end{cases} \tag{7}$$

where L_x, L_y and L_z correspond to the length of the projections of the sampling volumes in the main axes. Even though it is not known the exactly shape of the spatial weighting function *h(x,y,z)* implemented by the instrument within the sampling volume, a uniform distribution has been adopted. This assumption does not strongly affect the analysis presented in this paper, since Soulsby et al (1979) claimed that the signal attenuation is less sensitive to the form of the *h(x,y,z)* than to the size of the sampling volume.

Meanwhile considering also the temporal average, the equation (6) become in;

$$\mathrm{v(x,y,z,t)} = \frac{1}{N}\sum_{n=0}^{N-1}\frac{1}{JKI}\sum_{i=0}^{I-1}\sum_{j=0}^{J-1}\sum_{k=0}^{K-1} u(x+idx, y+jdy, z+kdz, t+\frac{n}{Nf_R}) \tag{8}$$

where f_R is the recording frequency implemented by the instrument.

Table 2 shows the height of the sampling volumes adopted for the spatial averaging analysis meanwhile the volumes adopted for the temporal analysis are presented in Table 3. The user-set frequencies used were: 247.8 [Hz]; 49.5 [Hz]; 24.7 [Hz], 9.9 [Hz] and 4.9 [Hz].

Units	Height of the sampling volumes			
	h_1	h_2	h_3	h_4
[mm]	1.50	3.00	6.00	9.00

Table 2: Sampling volumes for spatial averaging analysis.

Units	Height of the sampling volumes					
	h_1	h_2	h_3	h_4	h_5	h_6
[mm]	0.80	2.30	3.90	5.40	7.00	8.60

Table 3: Sampling volumes for temporal averaging.

After a set of synthetic velocity signals were extracted from the DNS, the sampled signals were analyzed in order to compute the corresponding turbulent parameters (mean values, Reynolds stresses, turbulent kinetic energy – TKE, autocorrelation function, power spectrum and time scales). Thus, the variation of these parameters can be evaluated as sampling volumes and sampling frequency change.

3 RESULTS

The consequences of the different sampling strategies are explored analyzing the effects in the parameters of turbulence. The dimensionless TKE, variances and one of the components of the Reynolds stress tensor are plotted as a function of the dimensionless parameter F defined for the temporal analysis as (Garcia et al, 2005),

$$F = \frac{H}{\frac{U_c}{f_R}} = \frac{f_T}{f_R} \tag{9}$$

where f_T = characteristic frequency of large eddies present in the flow, f_R = recording frequency, U_c = convective velocity and H = height of the flow. Meanwhile, as F increase, the relative values of the parameter of turbulence considered tend to 100% (Garcia et al. 2005). In the case of spatial averaging, F can also be defined as,

$$F_{sp} = \frac{z}{h_v} \tag{10}$$

where h_v = height of the sampling volumes and z = distance from the centre of the sampling volume to the bottom. The variables involved in the spatial and temporal analysis differ: the F in the temporal analysis is calculated considering only global flow variables; on the other hand in the spatial analysis F_{sp} is a combination of local variables.

3.1 Spatial averaging analysis

Figures 1, 2 and 3 show the effect of different sampling volumes on the TKE, variance in the longitudinal direction, and the Reynolds stress component involving the longitudinal and vertical directions. The turbulence parameters plotted in these figures are made dimensionless using the corresponding value of the parameter computed for the local value implying no spatial averaging. Those dimensionless parameters are plotted against F_{sp} calculated with Eq. (8). As the dimensionless number F_{sp} decrease, a bigger portion of energy is both filtered and aliased. The evolution of the variance in the main direction of the flow has the same behavior than one corresponding to the TKE. However, the evolution *uw* component presents a bigger dispersion than the other two parameters.

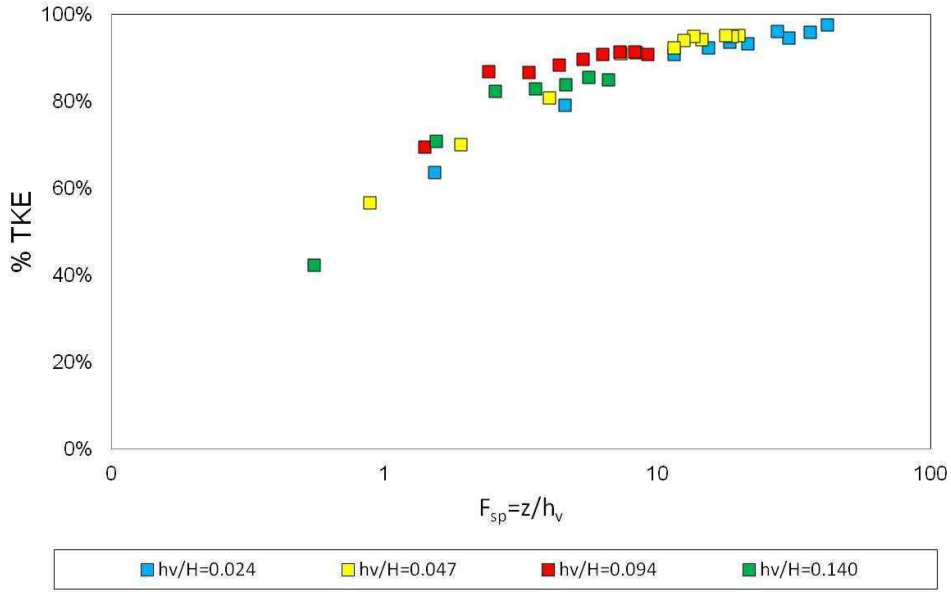

Figure 1: TKE remaining in the signal after spatial averaging for different z/H ratios.

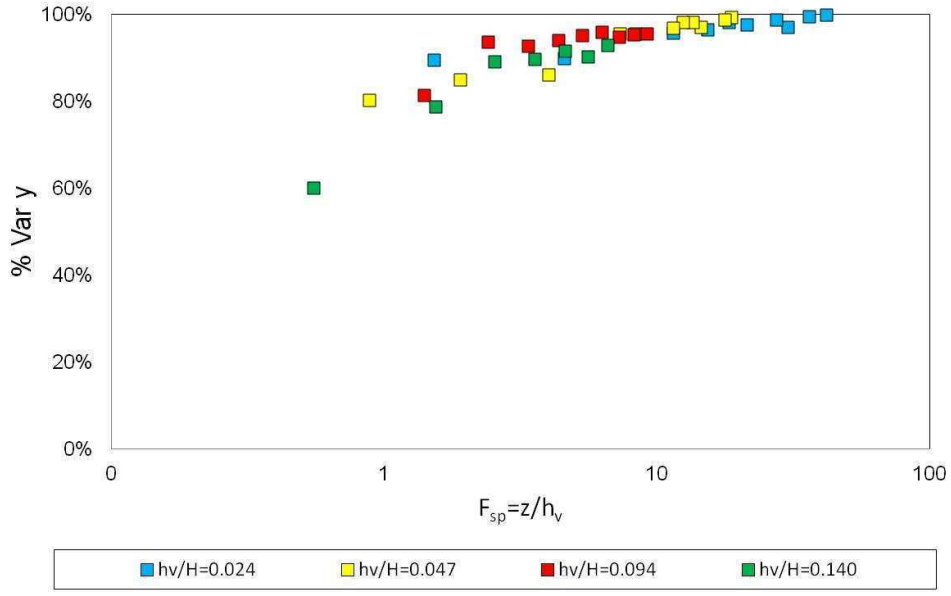

Figure 2: Variances in the main direction remaining in the signal after spatial averaging for different z/H ratios.

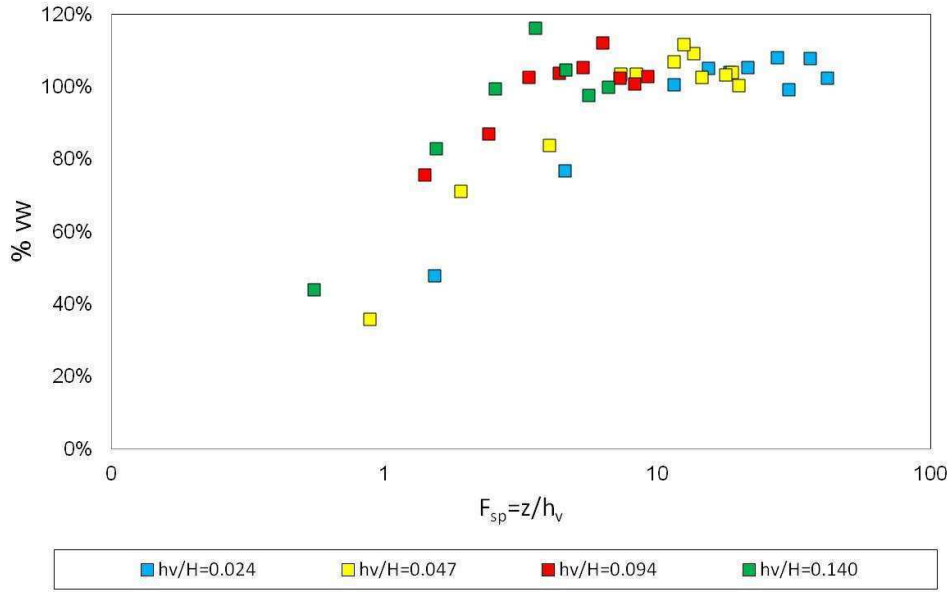

Figure 3: Reynolds stress component vw remaining in the signal after applying spatial averaging for different z/H ratios.

From the present analysis, it is concluded that a good sampling criterion should consider the values of $F_{sp}=z/h_v$ larger than 10, since such values yields reasonably small losses in the TKE and at the same time resolves important portions of the spectrum. The limit F=10 means, for example, that when using an Acoustic Doppler Velocimeter with a sampling volume of 4.5mm, turbulence cannot be accurately resolved in distance to the bottom closer than 4.5cm.

3.2 Spatial-temporal averaging analysis

This analysis consists of combining the spatial and temporal averaging as the instrument does while it measures the flow. When the two averaging are implemented together the adimensional parameter F adopted is the temporal, since the temporal averaging affects more the parameter of turbulence than the spatial averaging.

For the spatial-temporal analysis the data set considering three different distances to the bottom were considered. Each sampling volumes and location was sampled considering the user set frequencies f_R= 247.8 [Hz]; 49.5 [Hz]; 24.7[Hz], 9.8 [Hz] and 4.9 [Hz]. Then, values of TKE, variance in the longitudinal direction, and Reynolds stress component involving the longitudinal and vertical directions were made dimensionless using the corresponding value of the parameter computed for $f_R=f_s$=247.8 [Hz] in each depth (no temporal averaging). Figure 4 shows the evolution of the turbulence parameter, where it is plotted considering three different distances from the bottom and simulating six sizes of sampling volumes. As it can be observed (see Figure 4), three families of curves are presented, each of them representing a different distance to the bottom. It can be also seen the increasing influences of the sampling volume sizes in the variances as the measurements location come closer to the bottom of the channel. This means that the effect of the spatial averaging depends on the distance from the bottom of the channel. But since this effect is not considered in the dimensional frequency F,

the data is aligned vertically. Indeed *F* adimensional parameter should be calculated probably as a combination of the temporal and spatial averaging together.

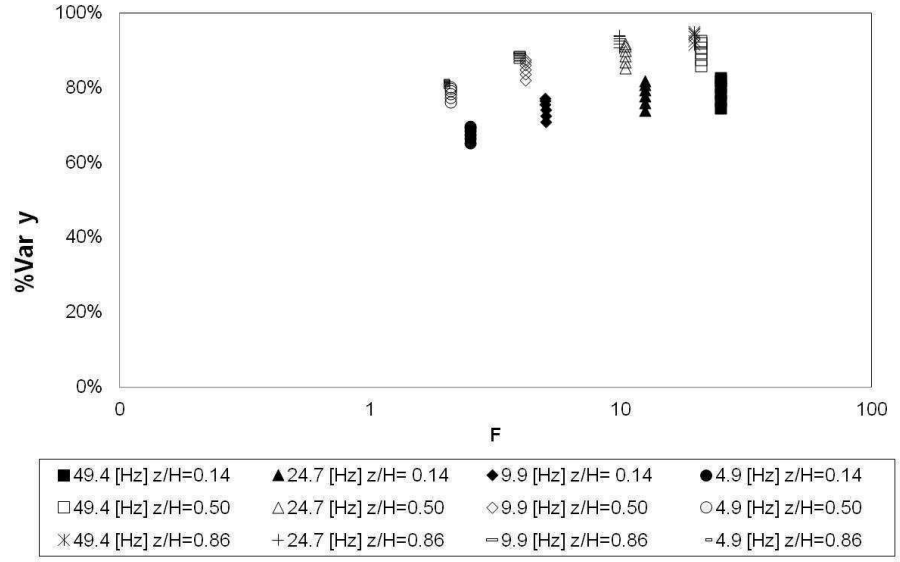

Figure 4: Evolution of the spatial and temporal averaging in the percentage of the variances in the main direction of the flow remaining in the signal against F for different location.

4 VALIDATION WITH EXPERIMENTAL DATA

In order to validated the DNS results, experimental specific data has been recorded in an open channel flow. The measurements were recorded in the hydraulic laboratory of National University of Litoral, Santa Fe, Argentina. First, a set of 60 three-dimensional water velocity time series were obtained with the down-looking Vectrino Nortek ADV of 10 MHz considering five different sampling volumes heights (h_v=2.5; 4; 5.5; 7 and 8.5 mm). Also five different recording frequencies values were adopted (f_R=100; 50; 25; 10; 5 Hz). The sampling volume of the velocimeter was located at z = 30 mm from the bottom of the channel. Three different flow conditions were analyzed (see Table 2).

The quality of the recorded signals is characterized by a correlation value in the range from 94 to 98 and a Signal to Noise Ratio (SNR) value in the range 39 to 48 dB, which are high enough values of these parameters to ensure good quality data. Additionally, experimental data presented in García et al. (2005) were also considered only en in the case of the variances in the main direction of the flow.

Conditions	Q [m^3/s]	H [m]	V [m/s]	B [m]
1	12.61	0.08	0.40	0.38
2	19.84	0.11	0.49	0.39
3	14.75	0.12	0.33	0.38

Table 2: Flow conditions for experimental data.

The first outstanding feature that can be observed in Figure 5 is that the results present a trend that agrees very well with the DNS results. The experimental data plotted in this figure were measured with f_R=100 [Hz] for three different flow conditions and five different sizes of volume measurements in order to minimize the temporal averaging. Experimental data with larger sampling frequencies did not present good quality (several spikes were present in the signal). Since the measurements were made for a fix distance to the bottom, the experimental data could not validate the entire range of F simulated by the DNS. Nevertheless the range of F_{sp} considered are the most common adopted during measurements.

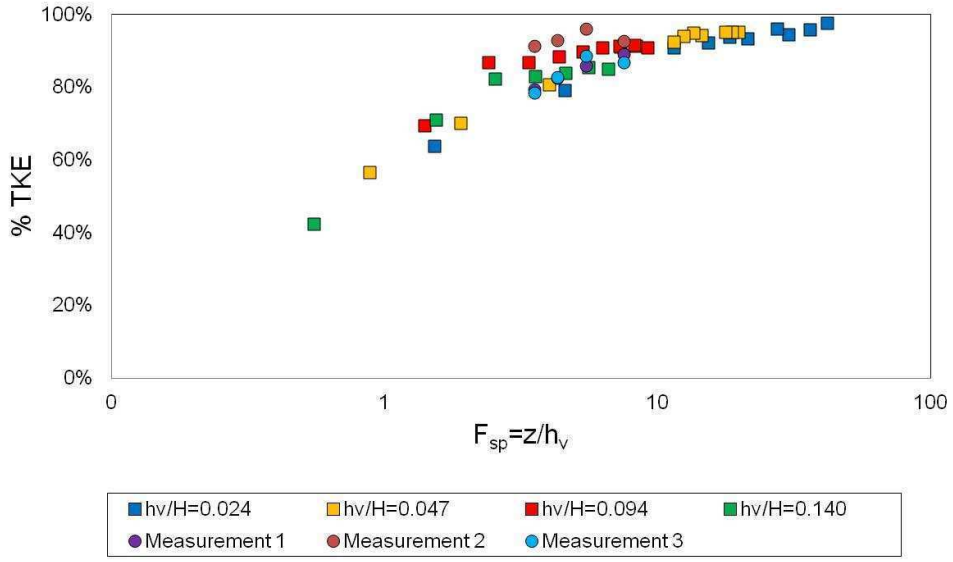

Figure 5: Validation of the DNS results with experimental data, which was measured with f_R=100 [Hz] for three different flow conditions and five different sizes of volume measurements.

Figure 6 shows a validation of both spatial and temporal averaging combined together. For this validation, the DNS result corresponding to z/H=0.14 and z/H=0.50 were used, since for the experimental data it was considered z/H=0.37. The experimental agrees very well with the DNS results.

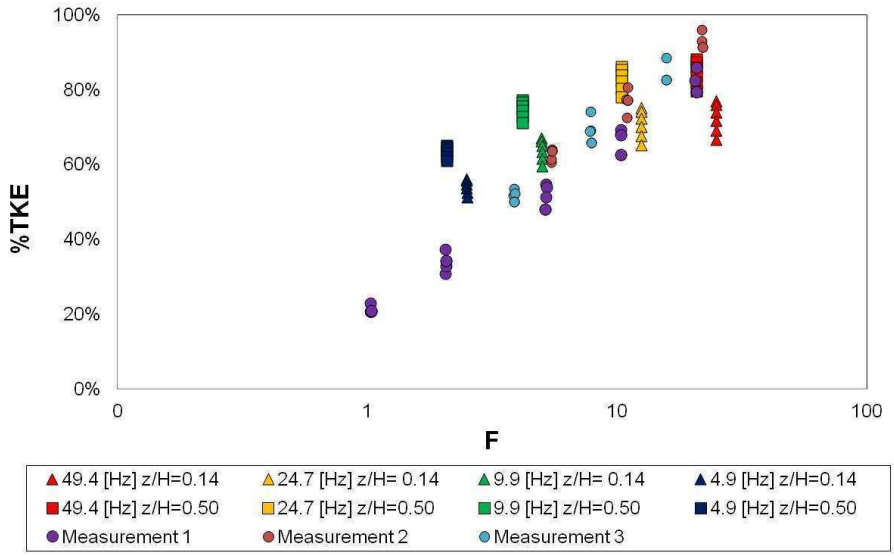

Figure 6: Validation of the DNS results considering both spatial and temporal averaging with experimental data.

5 CONCLUSIONS

Acoustic Doppler Velocimeters are able to accurately characterize turbulent flow if the right flow and sampling conditions are met during the measuring process. These considerations include the optimum determination of the sampling volume, sampling location and the recording frequency. ADVs technology biases low most of the parameters representative of turbulence as consequence of the spatial and temporal sampling averaging, however this effect may be neglected if the dimensionless frequencies F_{sp}>10 or F>20. This work presented an analysis of the effect of different sampling volumes and recording frequencies on the TKE, variance in the longitudinal direction, and the Reynolds stress component involving the longitudinal and vertical directions. The turbulence parameters plotted in these figures are made dimensionless using the corresponding value of the parameter computed for the local value implying no spatial averaging.

As the measurement location go deeper in the flow, the acoustic Doppler velocimeter should be operated at the maximum recording rate f_R and with the minimum sampling volume. However, the user has to be aware that this combination implies increasing the noise energy level presents in the signal.

The temporal averaging analysis performed in this work agrees with previous work (Garcia et al. 2005) that the temporal averaging acts as a low pass filter. However, the parameter F is calculated with global variables and all the transfer functions for a giving ratio between the sampling and recording frequencies are independently of the distance to the bottom. On the other hand the spatial averaging was demonstrated not to have the same transfer function depending on the distance to the bottom of the sampling volume. This is a direct consequence of the asymmetry of the sampling volume and the anisotropy and inhomogeneous nature of the turbulence. Thus the effect of the spatial averaging can not be represented by an equivalent low pass filter.

REFERENCES

Anderson S. y Lohrmann A. (1995). "*Open water test of the Sontek acoustic Doppler velocimeter*". Proc. IEEE Fifth Working Conf. on Current Measurements, St.Petersburg. FL. IEEE Oceanic Engineering Society . 188-192.

Bendat, J., and Piersol, A. (2000). "*Random data*". 3rd Ed., Wiley, New York.

Brown, D., Cortez, R. & Minion, M. (2001). "*Accurate projection methods for the incompressible navier-stokes equations*". Journal of Computational Physiscs 168, 464–499.

Cantero, M., Lee, J., Balachandar, S., and García, M. (2007a). "*On the front velocity of gravity currents*". Journal of Fluid Mechanics, Vol. 586, pp.1-39.

Cantero, M., Balachandar, S., and García, M. (2007b). "*High resolution simulations of cylindrical density currents*". Journal of Fluid Mechanics, Vol. 590, pp. 437-469.

Canuto, C., Hussaini, M.Y., Quarteroni, A., and Zang, T.A. (1988). "*Spectral Methods in Fluid Dynamics*". Springer, New York, U.S.A.

Cortese, T. & Balachandar, S. (1995) "*High performance spectral simulation of turbulent flows in massively parallel machines with distributed memory*". International Journal of Supercomputer Applications 9 (3), 187–204.

García C., Cantero M., Niño Y., and García M. (2005). "*Turbulence measurements with Acoustic Doppler Velocimeters*". J.Hydr. Engrg. ASCE. 131, 1062-1073.

Goring D., Nikora, V. (2002). "*Despiking Acoustic Doppler Velocimeter Data*". J. Hydr. Engrg. ASCE, Volume 128, (1), 117-126.

Hamming, R. (1983). "*Digital filters*". Second Edition. Prentice-Hall, Inc. New Jersey.

Kraus, N., Lohrmann, A., and Cabrera, R. (1994); "*New acoustic meter for measuring 3D laboratory flows*". J.Hydr.Engrg. ASCE. 120(3), 406-412.

Lane, S., Biron, P., Bradbrook, K., Butler, J., Chandler, J., Crowell, M., McLelland, S., Richards, K., and Roy, A. (1998) . "*Three-dimensional measurement of river channel flow processes using acoustic Doppler velocimetry*". Earth Surface Processes and Landforms. 23, 1247-1267.

Lemmin U. y Lhermitte R. (1999). "*Discussion of'ADV measurements of turbulence: Can we improve their interpretation*?' by Nikora,V., and Goring, D." J.Hydr. Engrg. ASCE. 125, 987-988.

Lohrmann, A., Cabrera R., and Kraus, N. (1994). "*Acoustic Doppler velocimeter (ADV) for laboratory use*". Proc. from Symposium on fundamentals and Advancements in Hydraulic measurements and Experimentation, ASCE. Buffalo. 351-365.

López, F., and Garcia, M. (2001). "*Mean flow structure of open-channel flow through non-emergent vegetation*" J.Hydr. Engrg. ASCE. 127(5), 392-402.

McLelland, S. and Nicholas, A. (2000). "*A new method for evaluating errors in high-frequency ADV measurements*". Hydrological Processes. 14, 351-366.

Nezu, I. (1977). "*Turbulence structure in open channel flows*". Ph.D Thesis. Kyoto University. Kyoto, Japan.

Nezu, I., and Nakagawa, H. (1993). "*Turbulence in open channels*". AA Balkema, Rotterdam, Holanda.

Nezu, I., and Rodi W. (1986). "*Open-Channel Flow Measurements with a Laser Doppler Anemometer*". Journal of Hydraulic Engineering, Vol. 112(5), pp. 335-355.

Nikora V. y Goring D. (1998). "ADV measuremets of turbulence: Can we improve their interpretation?" J.Hydr. Engrg. ASCE. 124, 630-634.

Romagnoli M., García M., Leopardo R., (2010) "*Signal Postprocessing Technique and Uncertainty Analysis of **ADV** Turbulence Measurements on Free Hydraulic Jumps",*

Journal of Hydraulic Engineering; Vol. 138 Issue 4, p353-357, 5p, 1 Chart, 5 Graphs.

Rusello, Peter; Lohrmann, Atle; Siegel Eric y Maddux, Tim. (2006). "*Improvements in Acoustic Doppler Velocimetery*". 7 th International Conference on Hydroscience and Engineering (ICHE-2006),Sep 10 –Sep 13,Philadelphia, USA.

Soulsby, R. (1979). "*Selecting Record Length and Digitization Rate for Near-Bed Turbulence Measurements*". Journal of Physical Oceanography. 10(2), 208–219.

SonTek (1997) "*Pulse coherent Doppler processing and the ADV Correlation*". SonTek Tech. Note, San Diego.

Voulgaris G., y Trowbridge J. (1998). "*Evaluation of the acoustic Doppler velocimeter (ADV) for turbulence measurements*". Journal of Atmospheric and Oceanic Technology. 15, 272-288.